Inorg. Chem. **1990**, *29*, 3110-3116

Contribution from the Department of Applied Chemistry, Faculty of Engineering, Kumamoto University, Kurokami, Kumamoto 860, Japan, and Institute for Molecular Science, Myodaiji, Okazaki 444, Japan

Ab Initio MO and SD–CI Study of $Ni(PH_3)_2(CO_2)$. Electron Correlation Effects on Geometry, Binding Energy, and Electronic Structure

Shigeyoshi Sakaki,*[1a] Nobuaki Koga,[1b] and Keiji Morokuma[1b]

Received November 21, 1989

Ab initio Hartree–Fock, single-reference single–double configuration interaction (SD–CI) and multireference SD–CI calculations were carried out for $Ni(PH_3)_2(CO_2)$. Introduction of electron correlation lengthens the $Ni-CO_2$ coordinate bond distance of the η^2-side-on complex and decreases the CO_2 binding energy. These correlation effects are opposite to those found in M(CO) (M = Ni, Pd, Pt), $Ni(PH_3)_2(\eta^1\text{-}N_2)$, and $Ni(PH_3)_2(C_2H_4)$. The difference in correlation effects between them comes from their different feature of the HOMO. The electronic structure of $Ni(PH_3)_2(\eta^2\text{-}CO_2)$ is analyzed in detail at the Hartree–Fock and SD–CI levels.

Introduction

Transition-metal–CO_2 complexes have recently drawn much attention, because coordination to transition-metal complexes is expected to activate an inert CO_2 molecule to undergo subsequent CO_2 fixation into organic substances.[2] In this regard, information concerning geometry, electronic structure, and reactivity of coordinated CO_2 molecule is indispensable. Several MO studies of transition-metal CO_2 complexes have been carried out,[3-6] in an attempt to obtain the above-mentioned information. Unfortunately, however, those MO papers were based on the Hartree–Fock (HF) level, and very little has been reported beyond the HF level.[7]

Very recently, Sakaki et al. have carried out a single–double configuration interaction (SD–CI) study of $Ni(PH_3)_2(N_2)$ and have reported several interesting electron correlation effects on geometry, binding energy, and relative stability of two coordination modes (η^1-end-on and η^2-side-on).[8] Such results of electron correlation effects indicate the necessity of reinvestigating a similar CO_2 complex, $Ni(PH_3)_2(CO_2)$, at the correlated level, which had been investigated previously with the ab initio MO method at the HF level.[3a]

In this work, ab initio MO and either single-reference or multireference SD–CI calculations are carried out for $Ni(PH_3)_2(CO_2)$. The electronic structural data, such as coordinate bond nature and electron distribution, are discussed first with energy decomposition analysis at the HF level and then discussed at the correlated level. Electron correlation effects on geometry and binding energy are also investigated.

Computation Details

Basis Sets and Geometries. An ab initio MO and SD–CI calculation was carried out with the MELD program,[9] while the energy decomposition analysis (EDA) study was performed with the IMSPACK program.[10] The MIDI-4 basis sets were used for C, O, and P atoms,[11] and the (4s/2s) set was employed for the H atom.[12] For Ni, Huzinaga's (13s7p5d) primitive set, proposed for the Ni $^3D(d^9s^1)$ state,[11] was augmented with a diffuse d primitive ($\zeta = 0.10$)[13] and three p primitives whose exponents were taken to be the same as the three most diffuse s primitives of Ni. The resultant (13s10p6d) primitive set was contracted to [5s4p3d], i.e., minimal for all core orbitals, double-ζ for the 4s and 4p orbitals, and triple-ζ for the 3d orbital.

The geometry of $Ni(PH_3)_2(\eta^2\text{-}CO_2)$ was taken from an X-ray experimental work for $Ni(PCy_3)_2(\eta^2\text{-}CO_2)$,[14] together with the experimental geometry of free PH_3.[15] Electron correlation effects on the coordinate bond distances were investigated by moving CO_2 along the z axis with the other geometrical parameters fixed, as shown in Figure 1. Correlation effects on the ligand distortion were examined by changing the OCO angle with the other part fixed.

The η^1-C coordinated $Ni(PH_3)_2(\eta^1\text{-}CO_2)$ was also investigated in an attempt to compare the relative stabilities of the η^2-side-on and η^1-C coordination modes. The $Ni(PH_3)_2$ part of this complex was assumed to have the same structure as in $Ni(PH_3)_2(\eta^2\text{-}CO_2)$. The geometry of the CO_2 part was optimized to have $R(C-O) = 1.21$ Å and $\angle OCO = 152°$ at $R(Ni-C) = 1.97$ Å with parabolic fitting of the total energy at the HF level,[16] where rather small basis sets were used for Ni and P atoms; (3s2p5d/2s2p2d) and (3s3p/2s2p) sets were employed to represent valence orbitals of Ni[17] and P[18] atoms, respectively, where the [Ar] core of Ni and the [Ne] core of P were replaced with effective core potentials.[17,18] Then, the Ni–C distance was optimized with the better basis sets described above.

Energy Decomposition Analysis at the HF Level. The electronic structure of molecular complexes can be successfully discussed at the HF level with the energy decomposition analysis method proposed by Morokuma et al.[19] In this analysis, the interaction energy (INT) is given as the stabilization energy of the complex relative to the distorted fragments, and the deformation energy (DEF) is defined as the destabilization energy to distort the CO_2 part to its deformed structure in the complex (the $Ni(PH_3)_2$ geometry is assumed to be fixed):

$$\mathrm{INT} = E_t[\mathrm{Ni(PH_3)_2(CO_2)}] - E_t[\mathrm{Ni(PH_3)_2}] - E_t(\mathrm{CO_2})_{\mathrm{dist}} \tag{1}$$

$$\mathrm{DEF} = E_t(\mathrm{CO_2})_{\mathrm{dist}} - E_t(\mathrm{CO_2})_{\mathrm{opt}} \tag{2}$$

The sum of INT and DEF is BE, which corresponds to the negative binding energy (be)

$$\mathrm{BE} = -\mathrm{be} = \mathrm{INT} + \mathrm{DEF} \tag{3}$$

INT is divided further into several chemically meaningful terms

$$\mathrm{INT} = \mathrm{ES} + \mathrm{EX} + \mathrm{FCTPLX} + \mathrm{BCTPLX} + R \tag{4}$$

where ES is the electrostatic term arising from the Coulomb interaction

---

(1) (a) Kumamoto University. (b) Institute for Molecular Science.

(2) For example: (a) Collin, J. P.; Sauvage, J. P. *Coord. Chem. Rev.* **1989**, *93*, 245. (b) Behr, A. *Angew. Chem., Int. Ed. Engl.* **1988**, *27*, 245. (c) Braunstein, P.; Matt, D.; Nobel, D. *Chem. Rev.* **1988**, *88*, 747. (d) Walther, D. *Coord. Chem. Rev.* **1987**, *89*, 135.

(3) (a) Sakaki, S.; Kitaura, K.; Morokuma, K. *Inorg. Chem.* **1982**, *21*, 760. (b) Sakaki, S.; Dedieu, A. *J. Organomet. Chem.* **1986**, *314*, C63. (c) Sakaki, S.; Dedieu, A. *Inorg. Chem.* **1987**, *26*, 3278. (d) Sakaki, S.; Aizawa, T.; Koga, N.; Morokuma, K.; Ohkubo, K. *Inorg. Chem.* **1989**, *28*, 103.

(4) Mealli, C.; Hoffmann, R.; Stockis, A. *Inorg. Chem.* **1984**, *23*, 56.

(5) Branchadell, V.; Dedieu, A. *Inorg. Chem.* **1987**, *26*, 3966.

(6) Rosi, M.; Sgamellotti, A.; Tarantelli, F.; Floriani, C. *Inorg. Chem.* **1987**, *26*, 3805.

(7) (a) The CO_2 binding energy of $RhCl(AsH_3)_4(\eta^1\text{-}CO_2)$ was calculated at the MP2 level.[3d] However, the details of electronic structure have not been investigated at the correlated level. (b) Dedieu, A.; Ingold, F. *Angew. Chem., Int. Ed. Engl.* **1989**, *28*, 1694.

(8) Sakaki, S.; Ohkubo, K. *J. Phys. Chem.* **1989**, *93*, 5655.

(9) Davidson, E. R.; McMurchie, L.; Elbert, S.; Langhoff, S. R.; Rawlings, D.; Feller, D. Program MELD. University of Washington, Seattle, WA; IMS computer center Library, No. 030.

(10) Morokuma, K.; Kato, S.; Kitaura, K.; Ohmine, I.; Sakai, S.; Obara, S. IMS computer center library, No. 0372.

(11) Huzinaga, S.; Andzelm, J.; Klobukowski, M.; Radzio-Andzelm, E.; Sakai, Y.; Tatewaki, H. *Gaussian Basis Sets for Molecular Calculations*; Elsevier: Amsterdam, 1984.

(12) Dunning, T. H.; Hay, P. J. Methods of Electronic Structure Theory; Schaefer, H. F., Ed.; Plenum: New York, 1977; p 1.

(13) This value was determined by even-tempered criterion.

(14) Aresta, M.; Nobile, C. F.; Albano, V. G.; Forni, E.; Manassero, M. *J. Chem. Soc., Chem. Commun.* **1975**, 636.

(15) Herzberg, G. *Molecular Spectra and Molecular Structure*; Academic Press: New York, 1967; Vol. 3, p 610.

(16) $R(Ni-C) = 1.97$ Å is the optimized value at $R(C-O) = 1.16$ Å and $\angle OCO = 151°$.

(17) Hay, P. J.; Wadt, W. R. *J. Chem. Phys.* **1985**, *82*, 270.

(18) Wadt, W. R.; Hay, P. J. *J. Chem. Phys.* **1985**, *82*, 284.

(19) (a) Morokuma, K. *Acc. Chem. Res.* **1977**, *10*, 294. (b) Kitaura, K.; Morokuma, K. *Int. J. Quantum Chem.* **1976**, *10*, 325. (c) Kitaura, K.; Sakaki, S.; Morokuma, K. *Inorg. Chem.* **1981**, *20*, 2292.

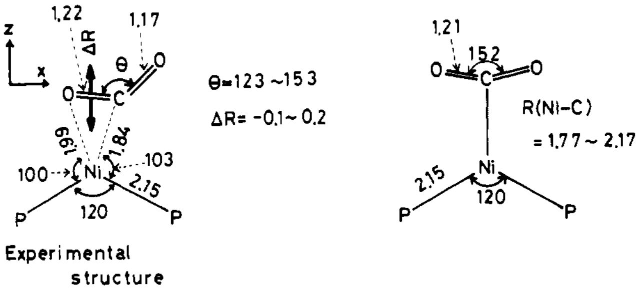

Figure 1. Geometries (in Å and deg) adopted for $Ni(PH_3)_2(\eta^2\text{-}CO_2)$[14] and $Ni(PH_3)_2(\eta^1\text{-}CO_2)$.

and EX is the exchange repulsion due to the Pauli exclusion principle. FCTPLX(B → A) includes a charge transfer from the ligand (B) to the metal fragment (A), a polarization of A, and their coupling term. BCTPLX(A → B) includes a charge back-transfer from A to B, a polarization of B, and their coupling term. R is a higher order coupling term. From the definition, a negative value means stabilization in energy for all these terms.

Configuration Interaction Calculations. SD–CI calculations were carried out with a single HF configuration as the reference, whereas virtual orbitals were transformed to K orbitals[20] to improve the CI convergence and all core orbitals were excluded from the active space. In $Ni(PH_3)_2(\eta^2\text{-}CO_2)$, about 332 500 spin-adapted configurations were screened, based on the second-order Rayleigh–Schrödinger perturbation theory (threshold = 5×10^{-5} hartree).[21] Resultant 26 000–27 700 spin-adapted configurations, which include over 93% of the estimated single–double correlation energy, underwent a variational SD–CI calculation. In the case of $Ni(PH_3)_2(\eta^1\text{-}CO_2)$, about 166 500 spin-adapted configurations were also subjected to the same perturbation selection and the resultant 17 000–19 900 spin-adapted configurations, which correspond to over 96% of the estimated single–double correlation energy, were used for the variational CI calculation. The coefficient of the reference configuration, C_0, is about 0.92 in all the complexes examined.

Only for the most important η^2-side-on complex, $Ni(PH_3)_2(\eta^2\text{-}CO_2)$, was a multireference (MR) SD–CI calculation carried out. In this calculation, the following three configurations were taken as references, $...(33a')^2(34a')^0$, $...(33a')^1(34a')^1$, and $...(33a')^0(34a')^2$, where 33a′ is a bonding orbital between Ni d_π and CO_2 π^* and 34a′ is its antibonding counterpart. The reason why these three were taken as references will be described later.

The variationally calculated limited SD–CI correlation energy, E_t(lim SD–CI), was corrected by estimating the correlation energy arising from the discarded configuration functions, to yield E_t(est SD–CI),[22a] and then further correction was carried out by estimating contributions of higher order CI expansions,[23] to give E_t(est full CI).[22b]

MP2 Calculations. MP2 calculations[24] were also carried out with the Gaussian 82 program,[25] as a preliminary investigation of electron correlation effects, where all core orbitals were excluded from the active space. The binding energy (be) of $Ni(PH_3)_2(\eta^2\text{-}CO_2)$ was, however, calculated to be significantly negative (this means significant destabilization); for instance, be = −29.7 kcal/mol at the experimental geometry. Furthermore, the total energy monotonously decreases upon increasing the $Ni-CO_2$ distance. Nevertheless, the binding energy is still considerably negative in the region of usual coordinate bond distance; even when CO_2 is moved away from Ni by 0.5 Å, the binding energy is still −18.3 kcal/mol. These unsuccessful results are quite similar to the previous results for $Ni(PH_3)_2(N_2)$ and $Ni(PH_3)_2(C_2H_4)$.[8] Thus, it seems to be a general trend that the MP2 method can not be applied to Ni(0) complexes.

Table I. Binding Energy and Coefficients of Some Leading Configurations

$Ni(PH_3)_2(\eta^2\text{-}CO_2)^a$

	SR SD–CI	MR SD–CI[c]	character of configuration
be,[b] kcal/mol	7.2	6.6	
C_0	$\underline{0.915}^c$	$\underline{0.909}^c$	
C_1	0.087	$\underline{0.121}$	$(Ni\ d_\pi + CO_2\ \pi^*)^2 \rightarrow (CO_2\ \pi^* - Ni\ d_\pi)^2$
C_2	0.073	$\underline{0.081}$	$(Ni\ d_\pi + CO_2\ \pi^*)^1 \rightarrow (CO_2\ \pi^* - Ni\ d_\pi)^1$
C_3	0.052	0.053	$CO_2\ (n\pi)^2 \rightarrow (\pi^*)^2$
C_5	0.036	0.038	$(Ni\ d_\pi + CO_2\ \pi^*)$, $Ni\ 3d_{xy} \rightarrow (CO_2\ \pi^* - Ni\ d_\pi)$, $Ni\ 4d_{xy}$
C_{14}	0.018	0.019	$Ni\ 3d_{xy}, 3d_{yz} \rightarrow Ni\ 4d_{xy}, 4d_{yz}$

$Ni(PH_3)_2(\eta^1\text{-}CO_2)^d$

	SR SD–CI	character of configuration
be,[b] kcal/mol	−0.4	
C_0	$\underline{0.915}^c$	
C_1	0.092	$(Ni\ d_\sigma + CO_2\ \pi^*)^2 \rightarrow (CO_2\ \pi^* - Ni\ d_\sigma)^2$
C_2	0.048	$(Ni\ d_\sigma + CO_2\ \pi^*)$, $Ni\ 3d_{xy} \rightarrow (CO_2\ \pi^* - Ni\ d_\sigma)$, $Ni\ 4d_{xy}$
C_3	0.046	$(Ni\ d_\sigma + CO_2\ \pi^*)$, $Ni\ 3d_{xz} \rightarrow (CO_2\ \pi^* - Ni\ d_\sigma)$, $Ni\ 4d_{xz}$
C_4	0.041	$(Ni\ d_\sigma + CO_2\ \pi^*)$, $Ni\ 3d_{yz} \rightarrow (CO_2\ \pi^* - Ni\ d_\sigma)$, $Ni\ 4d_{yz}$
C_5	0.041	$(Ni\ 3d_{xy})^2 \rightarrow (Ni\ 4d_{yz})^2$
C_6	0.027	$CO_2\ \pi, n\pi \rightarrow CO_2\ \pi^*, O\ 3p_\pi$
C_7	0.036	$CO_2\ \pi_\parallel, \pi_\perp \rightarrow \pi^*_\parallel, \pi^*_\perp{}^e$

[a] The experimental geometry. E_t(HF) = −2376.6973 hartrees, E_t(lim SD–CI) = −2377.2569 hartrees, E_t(est full CI) = −2377.4439 hartrees in the SR-SD–CI, and E_t(lim SD–CI) = −2377.2632 hartrees, E_t(est full CI) = −2377.4426 hartrees in the MR-SD–CI. [b] The binding energy at the estimated full CI level (kcal/mol). [c] Coefficients underlined are for reference configurations. [d] R(Ni–C) = 1.87 Å; see Figure 1 for the other geometrical parameters (this structure is very close to the optimized one obtained by parabolic fitting of total energies). E_t(HF) = −2376.6602 hartree, E_t(lim SD–CI) = −2377.2593 hartree, and E_t(est full CI) = −2377.4312 hartrees. [e] $\pi_\parallel$ is on the plane of $Ni-CO_2$ and $\pi_\perp$ is perpendicular to the plane. No marks mean the in-plane orbital.

Results and Discussion

Electron Correlation Effects on Geometry and Binding Energy. First, we shall compare MR SD–CI results with single reference (SR) SD–CI results for $Ni(PH_3)_2(\eta^2\text{-}CO_2)$ at the experimental structure. In the SR SD–CI calculation, the second and third leading electron configurations, $...(33a')^0(34a')^2$ and $...(33a')^1(34a')^1$, in addition to the reference, $...(33a')^2$, have rather large expansion coefficients, as shown in Table I. Therefore, these three configurations were taken as references in the MR SD–CI calculation. Compared to the SR SD–CI calculation, the MR SD–CI calculation yields, as expected, a slightly smaller C_0 but slightly larger C_1 and C_2 values. The binding energy[26] estimated with the MR SD–CI method is 6.6 kcal/mol, slightly smaller than that found with the SR SD–CI method (7.2 kcal/mol), as shown in Table I. These values of binding energy seem to be rather small for a normal-coordinate bond, which will be discussed later in

---

(20) Feller, D.; Davidson, E. R. *J. Chem. Phys.* **1981**, *84*, 3997.

(21) Langhoff, S. R.; Davidson, E. R. *Int. J. Quantum Chem.* **1974**, *8*, 61.

(22) (a) $E_t(\text{est SD–CI}) = E_0 + [E_t(\text{lim SD–CI}) - E_0](1 + E_{\text{discd}}/E_{\text{kept}})$, where E_0 is the total energy at the Hartree–Fock level and E_{discd} and E_{kept} are the SD correlation energy excluded and that included in the variational CI calculation, respectively. Both E_{discd} and E_{kept} are estimated by the second-order Rayleigh-Schrödinger perturbation method.

(23) Davidson, E. R.; Silver, D. W. *Chem. Phys. Lett.* **1977**, *52*, 403.

(24) (a) Moller, C.; Plesset, M. S. *Phys. Rev.* **1934**, *46*, 618. (b) Pople, J. A.; Binkley, J. S.; Seeger, R. *Int. J. Quantum Chem., Symp.* **1976**, *10*, 1. (c) Pople, J. A.; Krishnan, R.; Schlegel, H. B.; Binkley, J. S. *Int. J. Quantum. Chem.* **1978**, *14*, 545. (d) Krishnan, R.; Frisch, M. J.; Pople, J. A. *J. Chem. Phys.* **1980**, *72*, 4244.

(25) Binkely, J. S.; Frisch, M.; Reghavachari, K.; DeFrees, D.; Schlegel, H. B.; Whiteside, R.; Fluder, E.; Seeger, R.; Pople, J. A. *Gaussian 82*; Carnegie-Mellon Quantum Chemistry Archive; Carnegie-Mellon University: Pittsburgh, PA, 1983.

(26) (a) The binding energy was estimated as the energy relative to the structure where the $Ni(PH_3)_2-CO_2$ separation is 50 Å with R(C–O) = 1.16 Å, ∠OCO = 180°, and ∠PNiP = 120°. (b) At infinite separation, the $Ni(PH_3)_2$ fragment would have a linear structure (∠PNiP = 180°). The binding energy should be estimated as the difference from such a linear structure. However, it is not easy to calculate values for linear $Ni(PH_3)_2$, because low-lying states such as d^9s^1 must be taken into consideration. Even when a MR SD–CI calculation is applied, it is difficult to select reference configurations of the linear $Ni(PH_3)_2$ consistent with $Ni(PH_3)_2(CO_2)$. Thus, the binding energy was estimated as described in ref 26a. With this regard, the binding energy is meaningful in a comparison among $Ni(PH_3)_2(\eta^2\text{-}CO_2)$, $Ni(PH_3)_2(\eta^1\text{-}CO_2)$, and $Ni(PH_3)_2(C_2H_4)$.

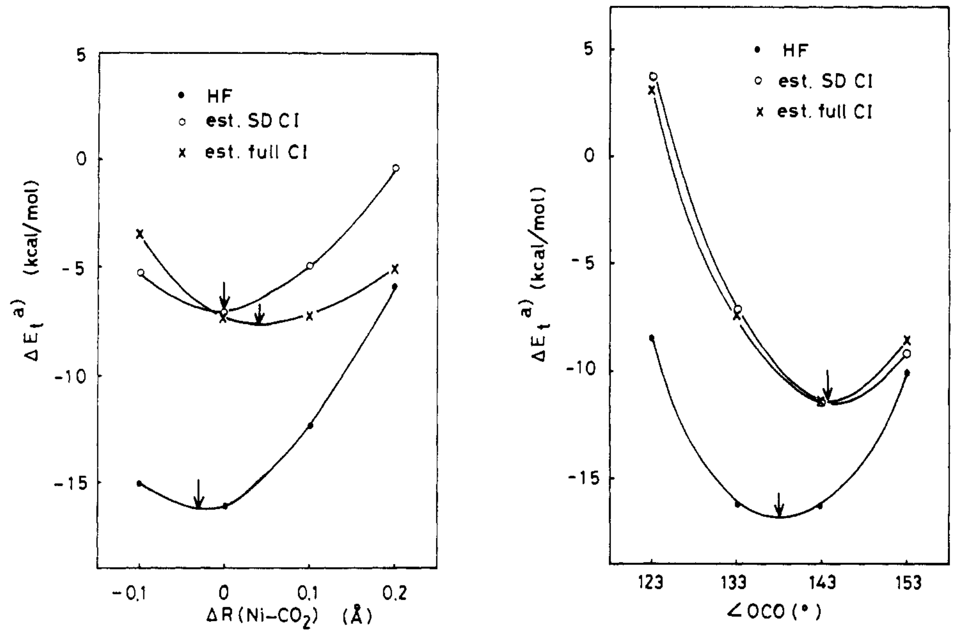

Figure 2. Relative energies[a] as functions of the Ni–CO$_2$ distance change, ΔR(Ni–CO$_2$),[b] and the OCO angle for Ni(PH$_3$)$_2$(η^2-CO$_2$). (a) The energy change ΔE is relative to structure at 50 Å separation between Ni and CO$_2$. (b) ΔR(Ni–CO$_2$) is the deviation of the CO$_2$ position from the experimental structure (see Figure 1).

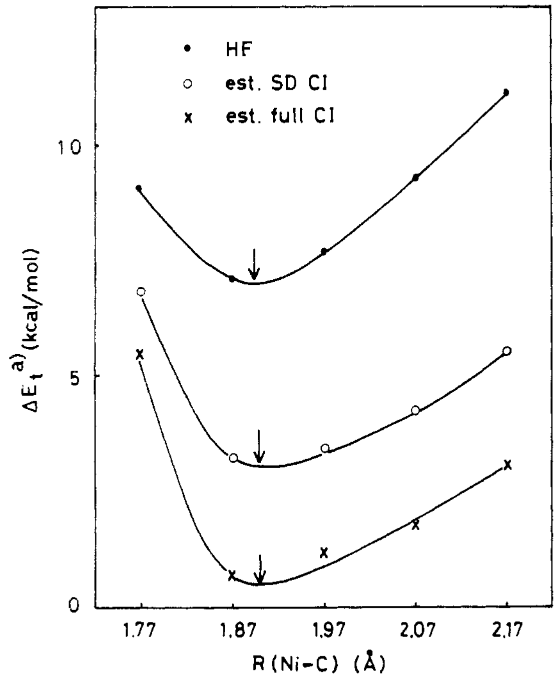

Figure 3. Relative energies as function of the Ni–C distance for Ni(PH$_3$)$_2$(η^1-CO$_2$).

detail. However, differences in the binding energy as well as the CI expansion coefficients are small between SR SD–CI and MR SD–CI calculations, indicating that this kind of Ni(0) complex can be investigated, at least semiquantitatively, with the SR SD–CI method.

Now, electron correlation effects on the Ni–CO$_2$ distance were examined in Ni(PH$_3$)$_2$(η^2-CO$_2$) by moving the CO$_2$ part away from the Ni atom along the z axis, with the other geometrical parameters fixed (see Figure 1). As shown in Table II and Figure 2, both HF and CI calculations give the Ni–CO$_2$ distance in good agreement with the experimental result.[14] It is noted that electron correlation effects lengthen the Ni–CO$_2$ distance by about 0.07 Å and decrease the binding energy significantly by about 10 kcal/mol. Although an analogous increase in the Ni–C$_2$H$_4$ distance upon introducing electron correlation effects has been found in our previous SD–CI study of a similar compound, Ni(PH$_3$)$_2$(C$_2$H$_4$),[8] the binding energy of C$_2$H$_4$ coordination increases with correlation effects. In Ni(PH$_3$)$_2$(η^1-CO$_2$), the Ni–C distance changes little, and the binding energy increases with correlation

Table II. Electron Correlation Effects on Geometry and Binding Energy[a]

compd	method	dev[b] from expt for R(Ni–CO$_2$), Å	binding energy,[c] kcal/mol
Ni(PH$_3$)$_2$(η^2-CO$_2$) (∠OCO = 133°)	HF	−0.03	17
	est SD–CI	0	7
	est full CI	0.04	8
compd	**method**	**dev[b] from expt for ∠OCO,[d] deg**	**binding energy, kcal/mol**
Ni(PH$_3$)$_2$(η^2-CO$_2$)	HF	138°	17
	est SD–CI	143°	12
	est full CI	143°	12
compd	**method**	**dev[b] from expt for R(Ni–C),[e] Å**	**binding energy, kcal/mol**
Ni(PH$_3$)$_2$(η^1-CO$_2$)	HF	1.90	−7
	est SD–CI	1.90	−3
	est full CI	1.90	−0.4
compd	**method**	**dev[b] from expt for R(Ni–C$_2$H$_4$),[f] Å**	**binding energy, kcal/mol**
Ni(PH$_3$)$_2$(C$_2$H$_4$)[g]	HF	1.81	29
	est SD–CI	1.85	33
	est full CI	1.89	35

[a] Values listed here are estimated from parabolic fitting of total energies. The total energy (hartrees) near the minimum are as follows. For Ni(PH$_3$)$_2$(η^2-CO$_2$) with the experimental structure, see footnote *a* of Table I. For Ni(PH$_3$)$_2$(η^2-CO$_2$), which has ∠OCO = 143°, E_t(HF) = −2376.6974, E_t(lim SD–CI) = −2377.2654, E_t(est full CI) = −2377.4504. For Ni(PH$_3$)$_2$(η^1-CO$_2$), which has R(Ni–C) = 1.87 Å, see footnote *d* of Table I. For Ni(PH$_3$)$_2$(C$_2$H$_4$), which has R(Ni–C$_2$H$_4$) = 1.90 Å and CH$_2$ bending = 26°, E_t(HF) = −2267.3074, E_t(lim SD–CI) = −2267.7888, and E_t(est full CI) = −2267.9432. [b] CO$_2$ is moved along the z axis with all the other geometrical parameters fixed (see Figure 1). A negative value means shortening of the Ni–CO$_2$ distance compared with the experimental structure and vice versa. [c] Defined as the energy at infinite (50 Å) separation minus the energy of the complex at the calculated minimum. [d] Only the OCO angle is altered, while the experimental Ni–CO$_2$ distance and the other parameters are fixed. [e] CO$_2$ is moved along the z axis with the rest of the geometry fixed. [f] The distance between the Ni atom and the center of the C=C bond. [g] Reference 8.

Chart I

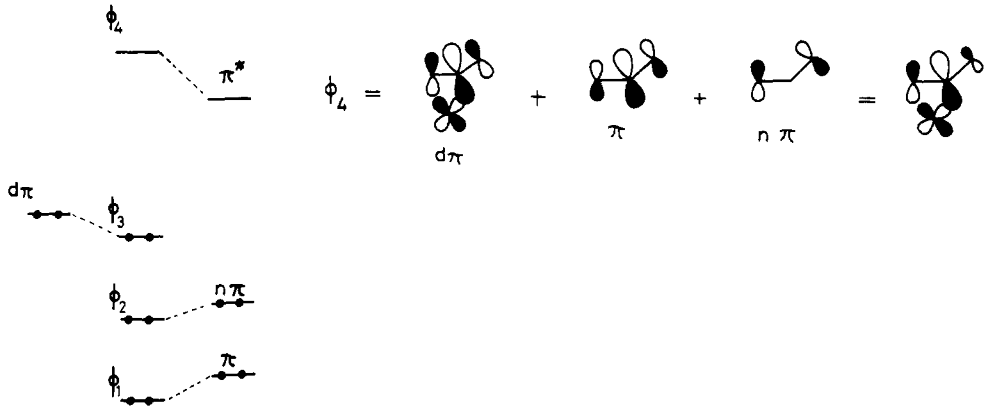

effects, as shown by Figure 3. The differences among η^2-CO_2, η^1-CO_2, and C_2H_4 complexes are considered to be related to their differences in electronic structure, as will be discussed later.

A highly distorted ligand is one of the characteristic features of low-valent non-Werner-type transition-metal complexes. Thus, electron correlation effects on the ligand distortion are worthy of examination. HF calculations result in the optimized OCO angle of 138°, slightly larger than the experimental value,[14] but correlation effects further increase the angle to 143° (see Table II and Figure 2).

The binding energy of the η^2-side-on mode is calculated to be 12 kcal/mol at the CI level for $\angle OCO = 143°$.[26] This value is reduced to about 5 kcal/mol after the correction for the basis set superposition error (BSSE) by the Boys method.[27a] One should note, however, that this method usually overcorrects the error.[27b] A rather small binding energy suggests that CO_2 binding in $Ni(PH_3)_2(\eta^2\text{-}CO_2)$ is weak. The binding energy of the η^1-C mode is estimated to be −0.4 kcal/mol (and −5.7 kcal/mol after BSSE correction) at the CI level. This repulsive interaction is consistent with the fact that the η^1-C mode has not been found experimentally in $Ni(PR_3)_2(CO_2)$.

Electronic Structure at the Hartree–Fock (HF) Level. First, the difference density at the HF level is analyzed with the EDA method of Morokuma et al.,[19] in order to clarify the nature of each interaction term such as EX, FCTPLX, BCTPLX, and *R*. The difference density maps of $Ni(PH_3)_2(\eta^2\text{-}CO_2)$ are given in Figure 4.[28] The EX term decreases the electron density in the region between Ni and CO_2, as expected for the exchange repulsion of electron clouds between $Ni(PH_3)_2$ and CO_2. The BCTPLX term decreases the electron density in the Ni d_π orbital but increases it in the CO_2 part, in particular on the O^t atom (the terminal O atom is denoted as O^t and the coordinate O atom as O^c). A significant accumulation of electron density on the O^t atom cannot be explained in terms of simple charge transfer from the Ni d_π to the CO_2 π^* orbital, because this simple charge-transfer interaction should increase the electron density more on the C atom than on the O atoms.[29] As discussed in a preceding section, the BCTPLX term includes some polarization in the CO_2 part. As shown in Chart I,[30] the unoccupied orbital ϕ_4 mainly consists of the CO_2 π^* orbital, into which the Ni dπ orbital mixes in an antibonding way. The CO_2 π and nonbonding π(nπ) orbitals furthermore exhibit antibonding mixing with the Ni dπ orbital.[31] As a result, the C p_π and O^c p_π orbitals contribute to this molecular orbital to a greater extent than the O^t p_π orbital. This means that in the occupied space the electron density accumulates more on the O^t atom than on the C atom.

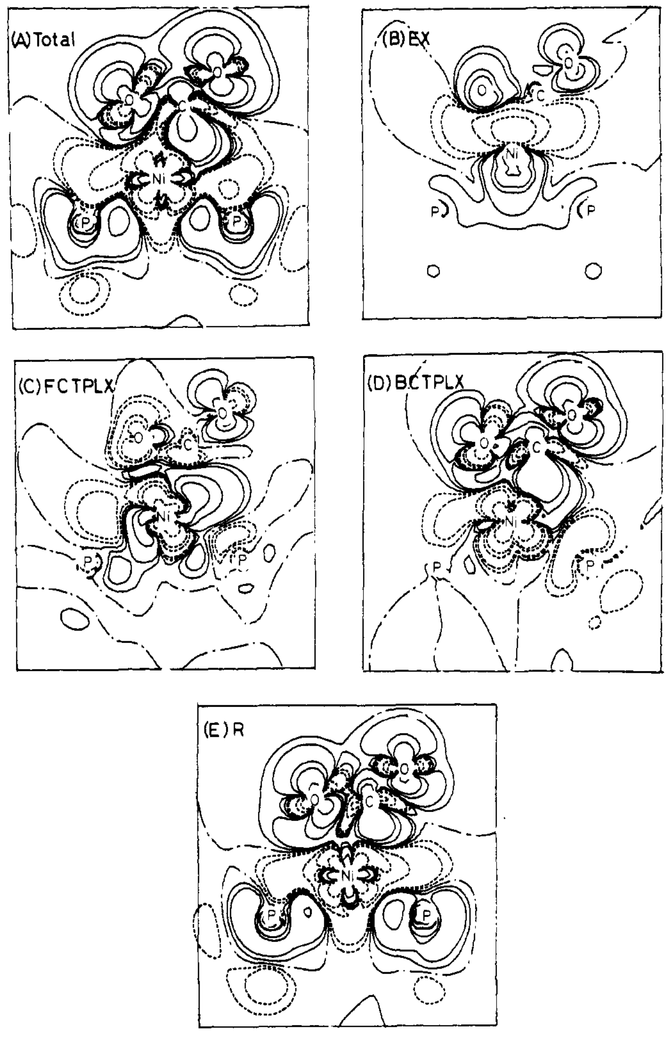

Figure 4. Total and EDA component difference density maps $\Delta\rho = \rho[Ni(PH_3)_2(\eta^2\text{-}CO_2)] - \rho[Ni(PH_3)_2] - \rho[CO_2]_{dist}$. $\Delta\rho = \pm0.05, \pm0.01, \pm0.005, \pm0.001, \pm0.0005$, and 0.0. Solid, dashed, and dashed–dotted lines show increases, decreases, and no change, respectively.

The FCTPLX term exhibits somewhat complicated features, as shown in Figure 4C. Considering that the FCTPLX term includes a charge transfer from CO_2 to $Ni(PH_3)_2$ and a polarization of the $Ni(PH_3)_2$ part, one might draw a coherent picture for this term. The charge-transfer interaction occurs from the CO_2 π and nπ orbitals to the $Ni(PH_3)_2$ part, which moves the electron density from C and O^c atoms to the region between the Ni and O^c atoms. The polarization of the $Ni(PH_3)_2$ part also takes place, in which electrons of the $Ni(PH_3)_2$ part are drawn toward the positively charged C atom and repelled from the negatively charged O^c atom.

---

(27) (a) Boys, S. F.; Bernardi, F. *Mol. Phys.* **1970**, *19*, 553. (b) For instance, Collins, J. R.; Gallup, G. A. *Chem. Phys. Lett.* **1986**, *123*, 56.

(28) Because this kind of difference density maps have been briefly discussed in our previous paper, we avoid the repetition here and take notice of only a few important results found in the present study.

(29) Note that the π^* orbital of CO_2 has a large C p_π and a small O p_π.

(30) In this chart, only orbital mixing in the virtual space is illustrated.[31] The electron distribution is given as a reverse of the virtual space orbital contribution.

(31) Inagaki, S.; Fujimoto, H.; Fukui, K. *J. Am. Chem. Soc.* **1976**, *98*, 4054.

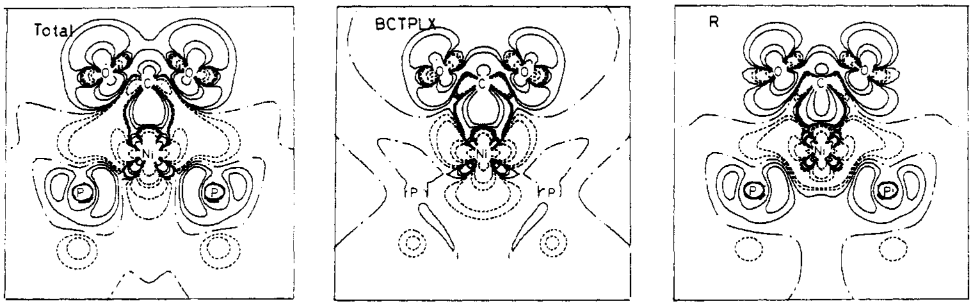

(A) $Ni(PH_3)_2(\eta^1-CO_2)$

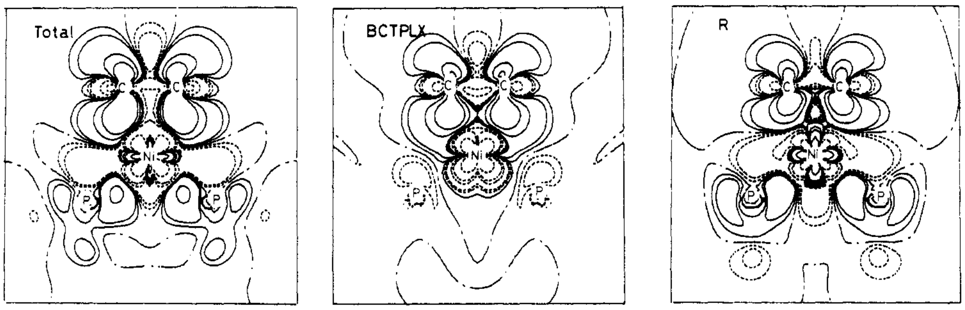

(B) $Ni(PH_3)_2(C_2H_4)$

Figure 5. Total, BCTPLX, and *R* component difference density maps for $Ni(PH_3)_2(\eta^1-CO_2)$ and $Ni(PH_3)_2(C_2H_4)$. See Figure 4.

The difference density map of the *R* term, which is a higher order term, exhibits several interesting results. (1) The electron density decreases in the region of the Ni, in particular the Ni dπ orbital, and increases in the region of the CO_2 part, which resembles very much the difference density map of the BCTPLX term. (2) At the same time, the electron density increases in the region of the PH_3 ligands, which suggests that some polarization occurs in the $Ni(PH_3)_2$ part. Very similar features are found in the difference density maps of $Ni(PH_3)_2(\eta^1-CO_2)$ and $Ni(PH_3)_2(C_2H_4)$, as shown in Figure 5 (compare the BCTPLX and *R* difference density maps between Figures 4 and 5). Although the character of the *R* term is in general ambiguous, these features strongly suggest that in these complexes the *R* term mainly consists of a coupling between charge back-transfer from Ni dπ to the L π^* orbital (L = CO_2, C_2H_4) and the $Ni(PH_3)_2$ polarization.

Now, let us discuss the nature of the coordinate bond from an energetic viewpoint. In all of these complexes, the BCTPLX stabilization is much larger than the FCTPLX stabilization, as compared in Table III. This means that the back-donating interaction contributes to the coordinate bond more than the donating interaction. $Ni(PH_3)_2(\eta^2-CO_2)$ exhibits several characteristic differences from a similar η^2-coordinated complex, $Ni(PH_3)_2(C_2H_4)$. (1) The BCTPLX and *R* stabilization of $Ni(PH_3)_2(\eta^2-CO_2)$ is remarkably large, which comes from the fact that the π^* orbital of the distorted CO_2 ligand lies much lower in energy than the π^* orbital of the distorted C_2H_4 ligand.[32] (2) The FCTPLX term yields a larger stabilization in $Ni(PH_3)_2(\eta^2-CO_2)$ than in $Ni(PH_3)_2(C_2H_4)$, probably owing to the presence of the nπ orbital of CO_2[33] in addition to the π orbital. (3) The ES stabilization is smaller in $Ni(PH_3)_2(\eta^2-CO_2)$ than in $Ni(PH_3)_2(C_2H_4)$, which is easily interpreted in terms of the Coulomb interaction of these complexes; the $Ni^{\delta+}-O^{\delta-}$ Coulomb attraction is weakened by the $Ni^{\delta+}-C^{\delta+}$ Coulomb repulsion in the η^2-side-on CO_2 complex, while in the C_2H_4 complex both $C^{\delta-}$ atoms can yield a Coulomb attraction with the $Ni^{\delta+}$ atom. (4) The DEF destabilization is larger in $Ni(PH_3)_2(\eta^2-CO_2)$ than in $Ni(PH_3)_2(C_2H_4)$, probably because the weak coordinate bond of CO_2 needs sufficient stabilization from π-back-bonding (note the CO_2 distortion lowers the π^* orbital energy, which favors the back-bonding). In other words, C_2H_4 does not need to cause a large distortion, because it has enough ability to coordinate to Ni(0) without a large distortion.

Table III. Energy Decomposition Analysis of the Interaction between $Ni(PH_3)_2$ and L (L = η^2-CO_2, η^1-CO_2, C_2H_4) (in kcal/mol)

	$Ni(PH_3)_2$-$(\eta^2-CO_2)^a$	$Ni(PH_3)_2$-$(\eta^1-CO_2)^b$	$Ni(PH_3)_2$-$(C_2H_4)^c$
BE	-16.2	7.9	-26.3
DEF	45.4	17.9	17.8
INT	-61.7	-10.2	-44.1
ES	-83.5	-31.6	-121.3
EX	146.3	65.2	147.6
FCTPLX	-21.7	-6.1	-8.5
BCTPLX	-76.7	-28.1	-50.7
R	-26.1	-9.6	-11.2

[a] The experimental structure.[14] [b] The structure is given in Figure 1. [c] $R(Ni-C_2H_4)$ = 1.9 Å, the optimized distance at the estimated full CI level.

$Ni(PH_3)_2(\eta^2-CO_2)$ also differs significantly from $Ni(PH_3)_2(\eta^1-CO_2)$. The latter receives smaller ES and BCTPLX stabilization because this mode suffers from the $Ni^{\delta+}-C^{\delta+}$ Coulomb repulsion and because the HOMO of $Ni(PH_3)_2$ is not the dσ orbital but the dπ orbital (note the Ni $d_\sigma \rightarrow CO_2\ \pi^*$ charge-transfer interaction is of importance in the η^1-C mode).[3b-d] This small BCTPLX stabilization would correspond to the small DEF destabilization. These small ES and BCTPLX stabilizations can not overwhelm the small EX repulsion and small DEF destabilization, and therefore, this mode is unstable in CO_2 coordination to $Ni(PH_3)_2$.

In conclusion, the electronic structure of $Ni(PH_3)_2L$ (L = η^2-side-on CO_2, η^1-CO_2, C_2H_4) is characterized by the strong back-donating interaction from the Ni d to the L π^*, coupled with polarizations of the L and $Ni(PH_3)_2$ parts.

Electronic Structure at the CI Level. Now, we are in a position to discuss the electronic structure at the SD–CI level. Several important configurations are listed with their CI expansion coefficients in Table I. The largest excited contribution comes from either $(\text{Ni } d_\pi + \text{L } \pi^*)^2 \rightarrow (\text{L } \pi^* - \text{Ni } d_\pi)^2$ in the η^2-side-on CO_2 and C_2H_4 complexes or $(\text{Ni } d_\sigma + \text{L } \pi^*)^2 \rightarrow (\text{L } \pi^* - \text{Ni } d_\sigma)^2$ in the η^1-CO_2 complex.[34] The next is either the CO_2 n$\pi \rightarrow \pi^*$

---

[32] The π^* orbital energy is 3.39 eV in the distorted C_2H_4 and 0.13 eV in the distorted CO_2, where the distorted structures were taken as in $Ni(PH_3)_2(\eta^2-CO_2)$ and $Ni(PH_3)_2(C_2H_4)$.

[33] The nπ orbital with the $Ni-CO_2$ plane lies at -13.98 eV and that perpendicular to this plane lies at -14.3 eV.

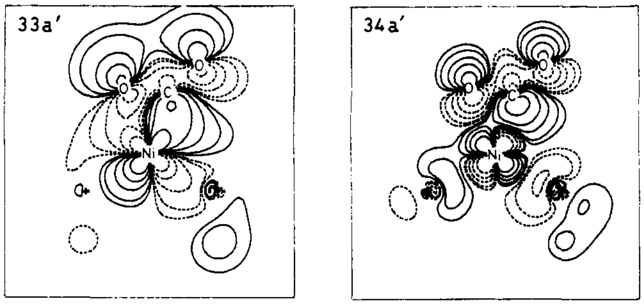

(A) $Ni(PH_3)_2(\eta^2\text{-}CO_2)$

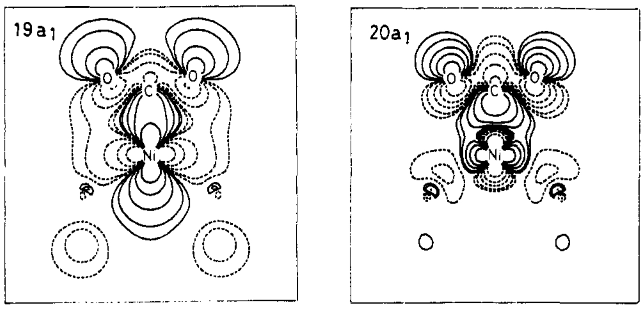

(B) $Ni(PH_3)_2(\eta^1\text{-}CO_2)$

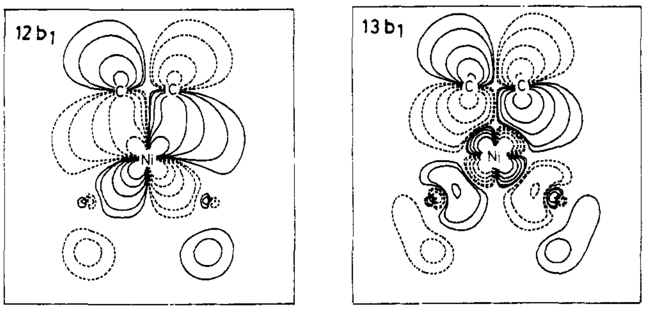

(C) $Ni(PH_3)_2(C_2H_4)$

Figure 6. Contour maps of several important natural orbitals for $\Delta\rho$ = ±0.2, ±0.1, ±0.05, ±0.02, and ±0.01.

excited configuration in the η^2-side-on complex or the Ni 3d → 4d excited configuration in the η^1-C complex.

Occupation numbers of several important natural orbitals are compared for the CO_2 complex and the infinitely (50 Å) separated structure in Table IV. Upon η^2-side-on CO_2 complexation, occupation numbers of natural orbitals change little in the a'' representation but considerably in the a' representation. This strongly suggests that the correlation of electrons in the a'' MO's is essentially intrafragmental, whereas the correlation of electrons in the a' MO's is directly related to the η^2-side-on CO_2 coordinate bond. The occupation number of the 33a' natural orbital decreases remarkably and that of the 34a' orbital increases significantly upon η^2-side-on CO_2 coordination. These two orbitals, pictured in Figure 6, apparently include a bonding overlap between Ni dπ and CO_2 π^* orbitals and its antibonding counterpart, respectively. In the η^1-C complex, the occupation number of the 19a$_1$ natural orbital decreases but that of the 20a$_1$ natural orbital increases signficantly upon CO_2 coordination. These orbitals are (Ni d_σ + CO_2 π^*) and (CO_2 π^* − Ni d_σ), respectively, as clearly shown in Figure 6B. From all these results about CI expansion coefficients and occupation numbers of natural orbitals, π-type back-bonding in $Ni(PH_3)_2(\eta^2\text{-}CO_2)$ or σ-type back-bonding in $Ni(PH_3)_2(\eta^1\text{-}CO_2)$ cannot be well described at the HF level but can be improved by introduction of electron correlation effects.

Table IV. Occupation Numbers for Several Important Natural Orbitals

(A) $Ni(PH_3)_2(\eta^2\text{-}CO_2)$

orbital	exptl R(Ni–C), Å	R(Ni–C) = 50 Å[b]
32a'	1.981 (CO_2 $\pi_\perp$, n$\pi_\perp$[c])	1.973 (CO_2 n$\pi_\perp$[c])
10a''	1.976 (CO_2 n$\pi_\parallel$)	1.977 (CO_2 n$\pi_\parallel$)
33a'	1.946 (Ni d_π + CO_2 π^*)	1.982 (Ni d_π)
34a'	0.061 (CO_2 π^* − Ni d_π)	0.038 (CO_2 $\pi^*_\parallel$)
11a''	0.031 (CO_2 $\pi^*_\perp$)	0.031 (CO_2 $\pi^*_\perp$)
35a'	0.018 (CO_2 $\pi^*_\parallel$)	0.017 (CO_2 $\pi^*_\parallel$)
12a''	0.016 (Ni 4d_{xy})	0.020 (Ni 4d_{xy})

(B) $Ni(PH_3)_2(\eta^1\text{-}CO_2)$

orbital	R(Ni–C) = 1.90 Å	R(Ni–C) = 50 Å
18a$_1$	1.983 (CO_2 $\pi_\perp$)	1.978 (CO_2 $\pi_\perp$)
6b$_2$	1.981 (CO_2 $\pi_\parallel$)	1.981 (CO_2 $\pi_\parallel$)
14b$_1$	1.978 (CO_2 n$\pi_\perp$)	1.974 (CO_2 n$\pi_\perp$)
4a$_2$	1.976 (CO_2 n$\pi_\parallel$)	1.976 (CO_2 n$\pi_\parallel$)
19a$_1$	1.954 (Ni d_σ + CO_2 π^*)	1.977 (Ni d_σ)
20a$_1$	0.056 (CO_2 π^* − Ni d_σ)	0.035 (CO_2 $\pi^*_\parallel$)
5a$_2$	0.017 (Ni 4d_{xy})	0.020 (Ni 4d_{xy})
8b$_1$	0.015 (Ni 4d_{yz})	0.018 (Ni 4d_{yz})

[a] The experimental structure (see Figure 1). [b] The Ni–CO_2 distance is lengthened by 50 Å with all the other geometrical parameters fixed. [c] See footnote *e* of Table 1.

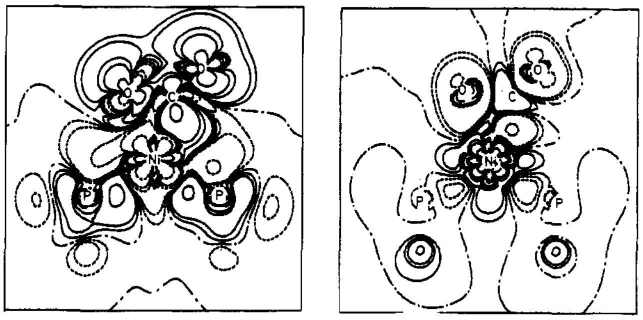

(A) Δ(Complex - ∞) on CI level (B) Δ(CI - HF)

$Ni(PH_3)_2(\eta^2\text{-}CO_2)$

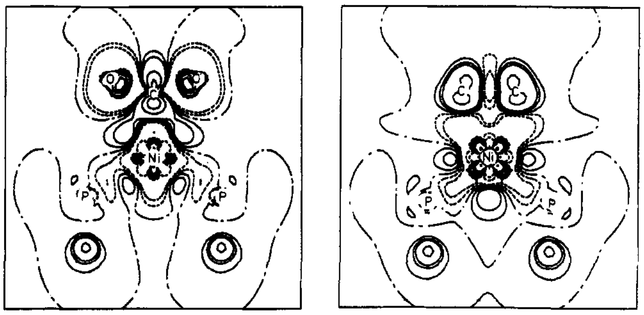

(C) $Ni(PH_3)_2(\eta^1\text{-}CO_2)$ Δ(CI - HF) (D) $Ni(PH_3)_2(C_2H_4)$ Δ(CI - HF)

Figure 7. CI difference maps ($\Delta\rho$(CI)) for the η^2-CO_2 complex, and the difference density between CI and HF levels (Δ(CI–HF)) for various complexes. $\Delta\rho(CI) = \rho(\text{complex}) - \rho(50\ \text{Å separated})$ at the CI level. $\Delta(CI\text{–}HF) = \rho_{CI} - \rho_{HF}$. See Figure 4 for values of contours.

It is worth examining the electron distribution at the CI level. The difference density map of $Ni(PH_3)_2(\eta^2\text{-}CO_2)$ at the CI level is shown in Figure 7A. This difference density map is essentially the same as that at the HF level (Figure 4A). Thus, the qualitative feature of the CO_2 coordinate bond can be described at the HF level. Of course, correlation effects have a nonnegligible influence on the electron distribution. As shown by a difference in the density between CI and HF levels (Figure 7B), electron correlation effects decrease the electron density in the region between the Ni and C atoms and in the region near the O atoms, but increase it in the regions near the C atom and Ni d_π orbital. Of these density changes, the change found in the CO_2 part is considered to come from the CO_2 intrafragmental electron correlation effects, because the CO_2 nπ → π^* excited configuration decreases electron density on the O atoms but increases it on the C atom. However, the density decrease found in the region between the Ni and C

---

(34) "a + b" and "a − b" mean the bonding and antibonding overlaps, respectively, between a and b orbitals, where the contribution of b is smaller than that of a.

atoms seems to result from the correlation effects on the Ni–CO_2 interaction. At the HF level, the density is increased in this region mainly by the back-bonding interaction (see Figure 4D). In other words, the back-bonding interaction increases the electron density between Ni and C atoms too much at the HF level, and correlation effects correct such an overestimated increase in the electron density. Essentially the same feature is found in $Ni(PH_3)_2(\eta^1\text{-}CO_2)$ and $Ni(PH_3)_2(C_2H_4)$; the difference density maps of Δ(CI–HF), in Figure 7C,D, show that electron accumulation at the HF level is decreased by correlation effects (see Figure 5 for the total difference density at the HF level).

In conclusion, correlation effects improve the description of the back-donating interaction in these complexes.

Understanding of Electron Correlation Effects on the Geometry and Binding Energy. There have been found two kinds of electron correlation effects on the coordinate bond distance; in one, the coordinate bond distance shortens upon introducing correlation, as exemplified by M(CO), $M(CO)_4$, (M = Ni, Pd, or Pt),[35] and $Ni(PH_3)_2(\eta^1\text{-}N_2)$.[8] In the other, the coordinate bond distance lengthens upon introducing correlation in $Ni(PH_3)_2(C_2H_4)$[8] and $Ni(PH_3)_2(\eta^2\text{-}CO_2)$. In organic compounds, the bond distance lengthens, in general, upon introducing electron correlation, which is understood by considering that excitations to antibonding orbitals contribute to the correlated wave function. In this regard, bond lengthening by electron correlation seems reasonable. In the case of $Ni(PH_3)_2(\eta^1\text{-}N_2)$, however, bond shortening has been found,[8] as described above, where the excited configuration to an antibonding ($N_2\ \pi^* - Ni\ d_\pi$) is the major contributor to the correlated wave function. A critical difference between the two cases is found in the occupied levels. In $Ni(PH_3)_2(\eta^1\text{-}N_2)$, the HOMO, which dominantly contributes to excited configurations, is nearly nonbonding, because three-orbital mixing of metal $d\pi$, ligand π, and π^* orbitals occurs.[8,36] On the other hand, the HOMO of $Ni(PH_3)_2(\eta^2\text{-}CO_2)$ and $Ni(PH_3)_2(C_2H_4)$ is strongly bonding between metal and ligand,[37] because the above-mentioned orbital mixing does not occur, owing to different symmetries of metal $d\pi$ and ligand π orbitals. From these results, electron correlation effects on the bond distance in the transition-metal complexes examined here seem to depend on the nature of the HOMO. In general, correlation effects would be expected to strengthen the metal–ligand interaction by incorporating the dispersion interaction, which would shorten the coordinate bond distance. When the HOMO is nearly nonbonding, this dispersion picture prevails, and the metal–ligand distance shortens by electron correlation. When the HOMO is strongly bonding, however, electron correlation reduces the bonding population and lengthens the coordinate bond distance. Thus, a balance of two different correlation effects on the bond length should be dependent on the nature of the HOMO.

The binding energy is expected to increase upon introducing electron correlation, as has been shown for M(CO), $M(CO)_4$ (M = Ni, Pd, Pt),[35] $Ni(PH_3)_2(\eta^1\text{-}N_2)$,[8] and $Ni(PH_3)_2(C_2H_4)$.[8] However, the binding energy of $Ni(PH_3)_2(\eta^2\text{-}CO_2)$ decreases upon introducing correlation effects, against the above-mentioned expectation. To clarify the reason, we compare two strong complexes: $Ni(PH_3)_2(\eta^2\text{-}CO_2)$ and $Ni(PH_3)_2(C_2H_4)$ (see Table II). As shown in Table I, the ($Ni\ d_\pi + CO_2\ \pi^*$) → ($CO_2\ \pi^* - Ni\ d_\pi$) excited configuration contributes significantly to the correlated wave function in $Ni(PH_3)_2(\eta^2\text{-}CO_2)$. A similar ($Ni\ d_\pi + C_2H_4\ \pi^*$) → ($C_2H_4\ \pi^* - Ni\ d_\pi$) excitation is important in $Ni(PH_3)_2(C_2H_4)$.[8] Therefore, the effect of interfragmental correlation on the M–L bond energy should be in the first approximation similar in both cases. The $Ni(PH_3)_2$ intrafragmental correlation would be similar as well. Thus, it is suspected that the major difference between the two complexes may come from the intrafragmental correlation of CO_2 and C_2H_4, both of which have received a substantial back-donation of electrons from the metal, as was shown and discussed with Table III. As a model of the back-donated ligand, the correlation energies of CO_2^- and $C_2H_4^-$ are calculated, and compared with those of CO_2 and C_2H_4. The SD-CI correlation energies (hartrees unit, after the Davidson correction) are 0.3392 for CO_2, 0.3136 for CO_2^-, 0.2113 for C_2H_4, and 0.2006 for $C_2H_4^-$. The correlation energy is lower for the anions than for the corresponding neutrals, and the decrease is larger for $CO_2 \rightarrow CO_2^-$ than for $C_2H_4 \rightarrow C_2H_4^-$. In CO_2 the correlation energy mainly comes from $n\pi \rightarrow \pi^*$ excitation, which is larger in magnitude and whose loss therefore causes a larger decrease than in C_2H_4 where the correlation mainly comes from $\pi \rightarrow \pi^*$ excitation. Furthermore, Table III shows that the CO_2 complex has a greater back-donation contribution than the C_2H_4 complex. Thus, the correlation energy is lost in η^2-side-on CO_2 coordination, resulting in net weakening of the M–L bond. In C_2H_4, presumably, the loss is more than compensated for by a gain of dispersion energy, an interfragmental correlation energy. $Ni(PH_3)_2(\eta^1\text{-}CO_2)$ is intrinsically a very weak complex, as shown in Table III, and the correlation energy should be mainly dispersion type, which should increase the binding energy.[38]

Concluding Remarks

In this theoretical work, ab initio MO, SR SD-CI, and MR SD-CI calculations were carried out for $Ni(PH_3)_2(\eta^2\text{-}CO_2)$, and several interesting correlation effects on CO_2 coordination were obtained. The most important excited configuration is the ($Ni\ d_\pi + CO_2\ \pi^*$) → ($CO_2\ \pi^* - Ni\ d_\pi$) in the η^2-side-on CO_2 complex and ($Ni\ d_\sigma + CO_2\ \pi^*$) → ($CO_2\ \pi^* - Ni\ d_\sigma$) in the η^1-CO_2 complex. This means the HF description of back-bonding is not good enough, and introduction of correlation effects improves the description.

The Ni–CO_2 distance is optimized at HF and SR SD–CI levels. Although both optimized values are in good agreement with the experimental distance, correlation effects lengthen the distance by ca. 0.07 Å. This result is opposite to the correlation effects on the coordinate bond distance previously found in M(CO) (M = Ni, Pd, Pt)[35] and $Ni(PH_3)_2(\eta^1\text{-}N_2)$.[8] The bond lengthening is interpreted in terms of the ($Ni\ d_\pi + CO_2\ \pi^*$) → ($CO_2\ \pi^* - Ni\ d_\pi$) excitation. Correlation effects on CO_2 binding energy is also against to our expectation; although the binding energy of coordination is expected to increase by correlation effects through incorporating dispersion interaction, binding energy between η^2-side-on CO_2 and $Ni(PH_3)_2$ is decreased by introducing correlation effects.

From the above results, we can obtain some qualitative prediction of the electron correlation effects on the binding energy, as follows: When the ligand has π and $n\pi$ orbitals at a high energy level and a strong π-back bonding is formed in $Ni(PH_3)_2L$, electron correlation stabilizes the Ni–L interaction to a lesser extent than the free ligand molecule, which decreases the binding energy of the coordinate bond.[38] The η^2-coordinate bond of NO_2^+ and CS_2 is expected to be such an example because they have the nonbonding π orbital as their HOMO, and a strong π-back-bond would be formed in their complexes. In ethylene, N_2, and CO, on the other hand, electron correlation would increase the binding energy because only the $\pi \rightarrow \pi^*$ excited configuration is important in these free molecules and π-back-bonding of these complexes is weaker than that in $Ni(PH_3)_2(\eta^2\text{-}CO_2)$. This kind of prediction would be useful in discussing the binding energy of large transition-metal complexes on which a CI calculation is difficult.

Acknowledgment. We gratefully acknowledge the Ministry of Education, Culture and Science for the Grand-in Aids for cooperative Research (No. 62303002) and the Computer Center, Institute for Molecular Science (IMS). This work was also supported by the Joint Studies Program (1988–1989) of IMS.

---

(35) Rohlfing, C. M.; Hay, P. J. *J. Chem. Phys.* **1985**, *83*, 4641.

(36) (a) Hoffmann, R.; Chen, M. M.-L.; Thorn, D. L. *Inorg. Chem.* **1977**, *16*, 503. (b) DuBois, D. L.; Hoffmann, R. *Nouv. J. Chim.* **1977**, *1*, 479.

(37) In the η^2-side-on coordination of CO_2, HOMO mainly consists of bonding overlap between the $Ni\ d_\pi$ and $CO_2\ \pi^*$ orbitals into which CO_2 π and $n\pi$ exhibit antibonding mixing with $Ni\ d_\pi$. In spite of such antibonding mixing of CO_2 π and $n\pi$, HOMO is still strongly bonding, because of a strong back-bonding interaction from Ni $d\pi$ to CO_2 π^*.

(38) The CO_2 binding energy in $Ni^IF(NH_3)_4(\eta^1\text{-}CO_2)$ increases upon introducing correlation effects in spite of its strong back-bonding, unlike $Ni(PH_3)_2(\eta^2\text{-}CO_2)$, because coordinate bonding nature and electron correlation in this complex significantly differs from $Ni(PH_3)_2(\eta^2\text{-}CO_2)$. Sakaki, S. To be published.